PNAS RESEARCH ARTICLE | IMMUNOLOGY AND INFLAMMATION

IL-33 controls IL-22-dependent antibacterial defense by modulating the microbiota

Ivo Röwekamp[a,1], Laura Maschirow[a,1], Anne Rabes[a,1], Facundo Fiocca Vernengo[a], Lutz Hamann[b], Gitta Anne Heinz[c], Mir-Farzin Mashreghi[c], Sandra Caesar[a], Miha Milek[d], Anna Carolina Fagundes Fonseca[b], Sandra-Maria Wienhold[a], Geraldine Nouailles[a], Ling Yao[a], Soraya Mousavi[b], Dunja Bruder[e,f], Julia D. Boehme[e,f], Monika Puzianowska-Kuznicka[g,h], Dieter Beule[d], Martin Witzenrath[a,i], CAPNETZ Study Group[2], Max Löhning[j,k], Christoph S. N. Klose[b], Markus M. Heimesaat[b], Andreas Diefenbach[b], and Bastian Opitz[a,i,3]

Edited by Staffan Normark, Karolinska Institutet, Stockholm, Sweden; received June 27, 2023; accepted April 22, 2024

IL-22 plays a critical role in defending against mucosal infections, but how IL-22 production is regulated is incompletely understood. Here, we show that mice lacking IL-33 or its receptor ST2 (IL-1RL1) were more resistant to *Streptococcus pneumoniae* lung infection than wild-type animals and that single-nucleotide polymorphisms in *IL33* and *IL1RL1* were associated with pneumococcal pneumonia in humans. The effect of IL-33 on *S. pneumoniae* infection was mediated by negative regulation of IL-22 production in innate lymphoid cells (ILCs) but independent of ILC2s as well as IL-4 and IL-13 signaling. Moreover, IL-33's influence on IL-22-dependent antibacterial defense was dependent on housing conditions of the mice and mediated by IL-33's modulatory effect on the gut microbiota. Collectively, we provide insight into the bidirectional crosstalk between the innate immune system and the microbiota. We conclude that both genetic and environmental factors influence the gut microbiota, thereby impacting the efficacy of antibacterial immune defense and susceptibility to pneumonia.

pneumonia | *Streptococcus pneumoniae* | microbiota | IL-33 | IL-22

Significance

Lower respiratory tract infections are the fifth leading cause of death. Here, we describe a mechanism influenced by genetic and environmental factors that affects the efficacy of pulmonary antibacterial immune responses. We show that IL-33 controls antibacterial defense by regulating the production of IL-22, a cytokine with known functions in antimicrobial immunity in the lungs. The effect of IL-33 on IL-22-dependent defense was influenced by the hygienic status of the mice and mediated by IL-33's modulatory effect on the animal's microbiota. In addition, genetic variation in genes involved in IL-33 signaling was associated with bacterial pneumonia in humans. Our findings may improve our understanding of the factors influencing predisposition to lower respiratory tract infections.

Lower respiratory tract infections are the most common infectious cause of death and the fifth leading cause of mortality overall (1). *Streptococcus pneumoniae* is the most frequently found pathogen in community-acquired pneumonia (CAP) (2, 3). The extracellular bacterium often asymptomatically colonizes the mucosal surfaces of the upper respiratory tract. Pneumonia only develops if pneumococci get access to the distal airways by aspiration and if they resist immediate elimination by the immune system (4, 5). The factors influencing the efficacy of antibacterial immune defense pathways in the lungs and thus determining susceptibility to pneumonia are, however, incompletely understood.

Antimicrobial immune responses to infections are initiated after sensing of microbial molecules by pattern recognition receptors (6, 7). This initiates release of chemokines and cytokines such as TNF-α, interleukin (IL)-1β, and IL-23, some of which induce subsequent production of additional cytokines including IFNγ and IL-22 by lymphoid cells (8). IL-22, which is primarily produced by type 3 innate lymphoid cells (ILCs), γδ T cells, and Th17 cells, is a mediator of immune defense against extracellular pathogens at mucosal organs (9–13). During pulmonary infections, IL-22 induces expression of antimicrobial peptides, tight junction proteins, and complement factors by lung epithelial cells and hepatocytes, respectively (14–17).

Alarmins such as HMGB1, IL-33, ATP, and uric acid are best known for their role as mediators of inflammation in response to sterile tissue damage (18). They are generally defined as endogenous danger molecules, which are normally hidden inside of host cells and only released upon cellular damage or stress. IL-33, for example, is stored in the nucleus of various stroma cells and is best known for its capacity to drive type 2 inflammation after release and binding to its transmembrane receptor ST2 (encoded by *IL1RL1*) (19). ST2 is expressed by, e.g., Th2 cells, ILC2s, and regulatory T cells but also by activated Th1 and $CD8^+$ cytotoxic T cells (20, 21). Moreover, a soluble form of ST2 (sST2) is generated by alternative polyadenylation, which lacks the transmembrane domain and binds IL-33 as a decoy receptor to prevent it from activating ST2 signaling (21, 22).

In our study, we initially aimed for a better understanding of the role of alarmins in regulating innate immune responses during bacterial infections. We demonstrate that IL-33 controls immune defense against *S. pneumoniae* in the lungs by influencing IL-22 production. Unexpectedly, however, we found that this mechanism was independent of ILC2s, IL-4, and IL-13. Instead, microbiota characterization by shotgun sequencing as well as functional cohousing, microbiota depletion, and transplantation experiments show

Preprint servers: This manuscript has been deposited as a preprint at bioRxiv (10.1101/2023.7.19.549679).

Author contributions: B.O. designed research; I.R., L.M., A.R., F.F.V., G.A.H., M.-F.M., S.C., A.C.F.F., S.-M.W., G.N., L.Y., S.M., D. Bruder, J.D.B., and M.M.H. performed research; M.P.-K., M.W., C.S.G., M.L., C.S.N.K., and A.D. contributed new reagents/analytic tools; I.R., L.M., A.R., L.H., M.M., and D. Beule analyzed data; I.R. visualized data; and I.R. and B.O. wrote the paper.

The authors declare no competing interest.

This article is a PNAS Direct Submission.

Copyright © 2024 the Author(s). Published by PNAS. This article is distributed under Creative Commons Attribution-NonCommercial-NoDerivatives License 4.0 (CC BY-NC-ND).

[1]I.R., L.M., and A.R. contributed equally to this work.

[2]A complete list of the CAPNETZ Study Group can be found in the *SI Appendix*.

[3]To whom correspondence may be addressed. Email: bastian.opitz@charite.de.

This article contains supporting information online at https://www.pnas.org/lookup/suppl/doi:10.1073/pnas.2310864121/-/DCSupplemental.

Published May 23, 2024.

that IL-33's influence on *S. pneumoniae* infection was mediated by its modulatory effect on the microbiota.

Results

IL-33 Enhances Susceptibility to *S. pneumoniae*–Induced Pneumonia. To better understand how the immune response to *S. pneumoniae* is regulated, we first investigated whether alarmins were released during infection. We detected increased levels of uric acid, ATP, and IL-33 in the supernatants of macrophages, alveolar epithelial cells (AECs), and/or lung tissue explants upon infection with *S. pneumoniae* in vitro (*SI Appendix*, Fig. S1 *A–C*). Next, we tested whether these alarmins affect pneumococcal pneumonia in vivo. As assessed 48 h after intranasal infection, neither degradation of uric acid or ATP nor inhibition of or deficiency in nucleotide receptors influenced bacterial loads (*SI Appendix*, Fig. S1 *D–G*). In contrast, lack of IL-33 or ST2 rendered mice more resistant to *S. pneumoniae*, as indicated by improved bacterial control (Fig. 1 *A*, *B*, *D*, and *E*) and reduced body temperature decrease (Fig. 1 *C* and *F*). Bone marrow chimera experiments, using WT or *Il33*$^{-/-}$ mice as either donors or recipients of bone marrow transplants, indicated that the detrimental effect of IL-33 during pneumococcal infection depended on its expression in recipient animals rather than the transplanted bone marrow (Fig. 1 *G* and *H*). In addition, we analyzed single-nucleotide polymorphisms (SNPs) previously associated with type 2 inflammation and altered sST2 or IL-33 levels (22–27) in 238 pneumococcal pneumonia patients and 238 age- and sex-matched controls. We found that SNP alleles previously linked to lower levels of the decoy receptor sST2 (22, 23), and by trend a SNP allele recently associated with higher IL-33 levels (24), were more frequent in the pneumonia patients as compared to the controls (*SI Appendix*, Fig. S2 *A–D*). Overall, our results demonstrate that IL-33 influences susceptibility to pneumococcal pneumonia in mice and possibly in humans.

Lack of ILC2s Does Not Influence Susceptibility to *S. pneumoniae*. To characterize the mechanism underlying the enhanced resistance of IL-33-deficient mice to *S. pneumoniae*, we first examined their inflammatory immune response. We did not observe any influence of IL-33 deficiency on levels of chemokines and various cytokines in bronchial alveolar lavage fluid (BALF) (*SI Appendix*, Fig. S3*A*), nor did we observe an effect on numbers and proportions of alveolar macrophages (AMs), polymorphonuclear neutrophils (PMNs), and inflammatory monocytes (*SI Appendix*, Fig. S3 *B–D*). Next, we performed single-cell RNA sequencing (scRNAseq) of pulmonary cells from *S. pneumoniae*–infected mice. We enriched the total lung cells (3/4) with fluorescence-activated cell sorting (FACS) lineage$^-$ CD90.2$^+$ CD127$^+$ cells (1/4) to also enable analysis of scarcer ILCs. Cellular populations were visualized by Uniform Manifold Approximation And Projection (UMAP) (*SI Appendix*, Fig. S4*A*) and classified based on signature genes (*SI Appendix*, Fig. S4*B*). We found *IL1RL1* to be primarily expressed by ILC2s (Fig. 2*A*). In addition, we defined subclusters for AMs, PMNs,

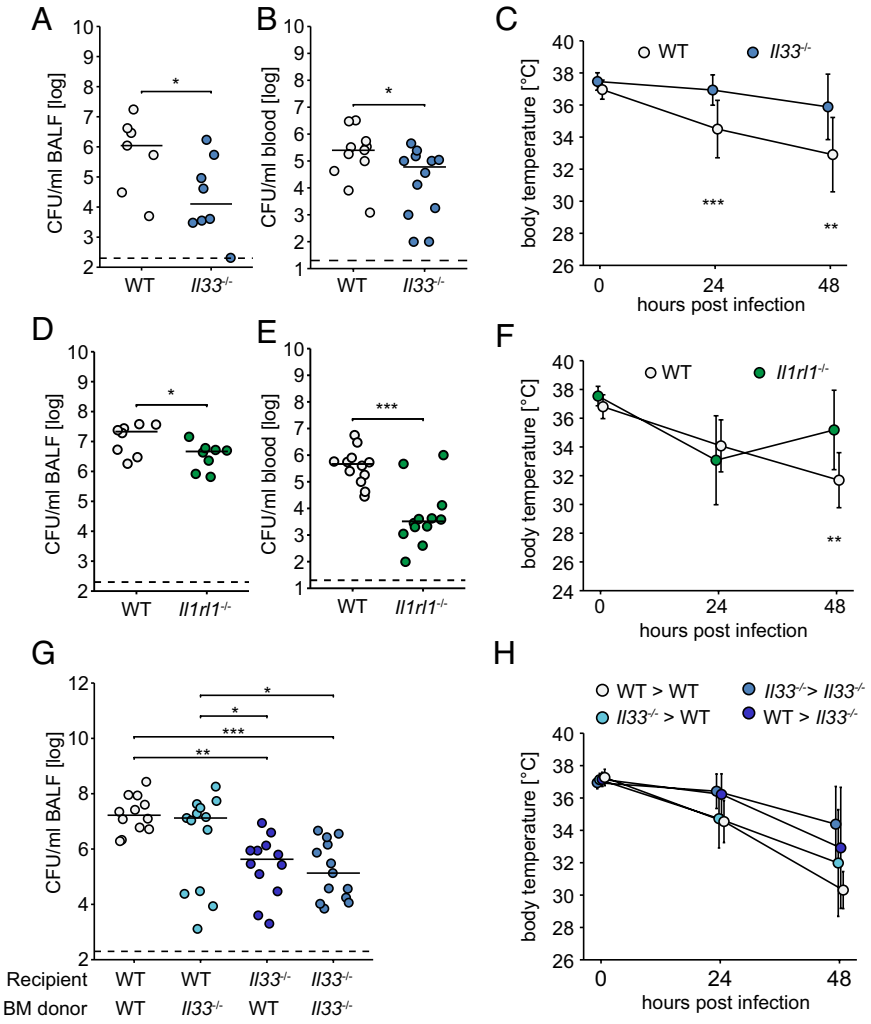

Fig. 1. IL-33 deficiency enhances the resistance of mice to pneumococcal pneumonia. WT (n = 11) and *Il33*$^{-/-}$ (n = 12) mice were intranasally infected with 5 × 10^6 CFU/mouse of *S. pneumoniae* and bacterial loads in BALF (*A*) and blood (*B*) were determined 48 h postinfection, and temperature was measured at the indicated time points (*C*). (*D–F*) WT (n = 12) and *Il1rl1*$^{-/-}$ (n = 12) were infected and bacterial loads in BALF (*D*) and blood (*E*) were determined 48 h postinfection, and temperature was measured (*F*). (*G* and *H*) Bone marrow chimeras (n = 12 per group) were infected and bacterial loads in BALF were determined 48 h postinfection (*G*), and temperature was measured (*H*). (*A*, *B*, *D*, *E*, and *G*) Data are shown as individual points. Lines represent the median and the dashed line the lower detection limit. The Wilcoxon rank-sum test or Kruskal–Wallis followed by Dunn's post hoc test was used if more than two groups were compared. (*C*, *F*, and *G*) Data are shown as mean ± SD, Kruskal–Wallis followed by Dunn's post hoc test; *P < 0.05, **P < 0.01, and ***P < 0.001.

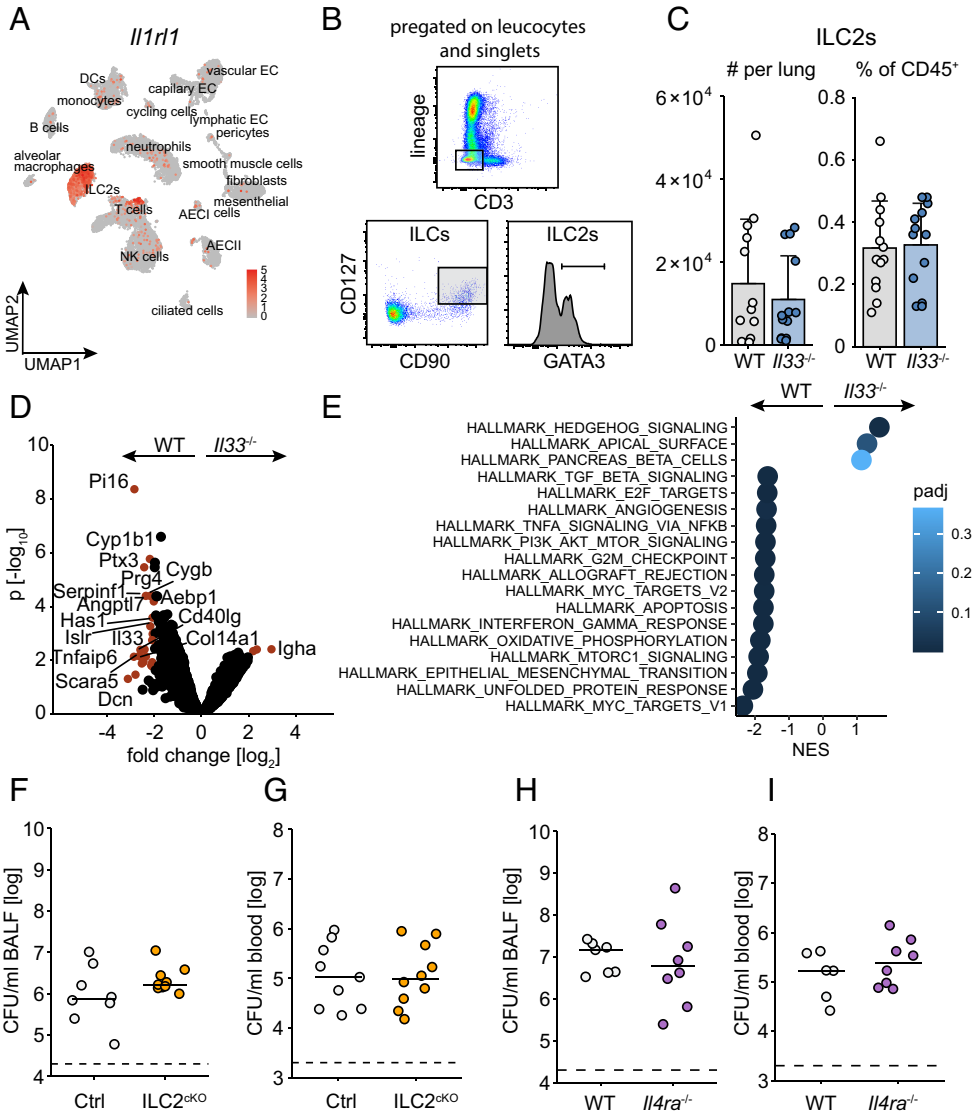

Fig. 2. ILC2 as well as IL-4 and IL-13 signaling do not regulate early antibacterial defense during pneumococcal pneumonia. (*A*) WT and *Il33*$^{-/-}$ mice were infected with *S. pneumoniae* and killed after 18 h, and pulmonary cells were analyzed by scRNAseq (pulmonary cells were pooled from n = 4 per group). Normalized expression levels of *Il1rl1* were plotted in an UMAP embedding. (*B*) Gating strategy to quantify ILC2s by FACS. (*C*) Numbers and frequencies of pulmonary Lin$^-$ CD90$^+$ CD127$^+$ GATA3$^+$ ILC2s from the lungs of WT (n = 12) and *Il33*$^{-/-}$ mice (n = 13) 18 h after infection. Bars represent mean + SD. (*D* and *E*) The lungs of 3 to 4 mice per group were digested at 12 h postinfection and sorted for ILC2s, and RNA was isolated and analyzed using bulk RNA sequencing. (*D*) Volcano plot displaying differentially expressed genes (DEGs) in ILC2s of WT and *Il33*$^{-/-}$ animals. Significant DEGs with a log2FC threshold of ± 2 and an adjusted *P* value of < 0.05 are indicated in red. (*E*) GSEA analysis utilizing HALLMARK collection, normalized enrichment score (NES), and adjusted *P*-values (padj) are indicated. (*F* and *G*) *Nmur1*$^{iCre\text{-}eGFP}$*Id2*$^{fl/fl}$ mice (ILC2^{cKO}) (n = 9) and littermate controls (n = 10) were infected, and bacterial loads in BALF and blood were assessed 48 h post infection. (*H* and *I*) *Il4ra*$^{-/-}$ (n = 7) and WT mice (n = 8) were infected, and bacterial loads in BALF (*H*) and blood (*I*) were assessed at 48 h postinfection. Data are shown as individual points. Lines represent the median and the dashed line the lower detection limit.

and monocytes based on unbiased clustering but did not observe differences in their relative abundance between WT and *Il33*$^{-/-}$ mice (*SI Appendix*, Fig. S4 *C–K*).

Since the IL-33 receptor was mainly expressed by ILC2s, we next compared their numbers and proportions in WT and *Il33*$^{-/-}$ mice, without identifying differences (Fig. 2 *B* and *C*). Next, we investigated their gene expression by bulk RNAseq. Several genes including, for example, *Pi16*, *Cyp1b1*, and *Tnfaip6* and gene sets such as "HALLMARK_MYC_TARGETS" showed decreased expression in *Il33*$^{-/-}$ as compared to WT mice during *S. pneumoniae* infection (Fig. 2 *D* and *E*). Early control of *S. pneumoniae* infection was, however, unchanged in mice specifically lacking ILC2s (*Nmur1*$^{iCre\text{-}eGFP}$*Id2*$^{fl/fl}$) (28, 29) or in animals deficient in IL-4 and IL-13 signaling (*Il4ra*$^{-/-}$) (Fig. 2 *F–I*). Thus, unlike IL-33 and ST2, ILC2s or the type 2 inflammation–associated cytokines IL-4 and IL-13 do not regulate early antibacterial defense against *S. pneumoniae* during lung infection.

The Protective Effect of IL-33 Deficiency in Pneumococcal Infection Is Mediated by Enhanced IL-22 Production. IL-22 is an important mediator of antibacterial immune defense at mucosal barriers such as the lungs (30, 31). We noticed enhanced IL-22 production in *Il33*$^{-/-}$ animals as compared to WT controls upon infection with *S. pneumoniae* (Fig. 3*A*). Bone marrow chimera experiments indicated that the influence of IL-33 on IL-22 production depended on its expression in recipient animals (*SI Appendix*, Fig. S5*A*). In line with this observation, we found a significant increase in the proportions and numbers of IL-22-producing ILCs in the lungs of infected *Il33*$^{-/-}$ mice, which were ST2-negative and most likely represented ILC3s, but we did not observe differences in IL-22 production by αβ and γδ T cells (Fig. 3 *B–D*). In order to test whether the enhanced production of IL-22 was responsible for the increased resistance of *Il33*$^{-/-}$ mice to *S. pneumoniae* infection, we generated *Il33*$^{-/-}$*Il22*$^{-/-}$ double knockout mice and compared them with *Il33*$^{-/-}$, *Il22*$^{-/-}$, and WT animals. We observed that the bacterial loads in the lungs and blood of *Il33*$^{-/-}$*Il22*$^{-/-}$ mice were largely similar compared to the ones in WT mice and significantly higher than in *Il33*$^{-/-}$ mice (Fig. 3 *E* and *F*). Moreover, treatment with rIL-22 enhanced the resistance of WT animals to *S. pneumoniae* infection (*SI Appendix*, Fig. S5*B*). These results indicate that increased production of IL-22 is responsible for the enhanced resistance of IL-33-deficient mice to pneumococcal lung infection.

The Effect of IL-33 Deficiency on Pneumococcal Infection Depends on the Vivarium in Which the Mice Were Bred. For operational reasons, the breeding of our *Il33*$^{-/-}$ and WT control

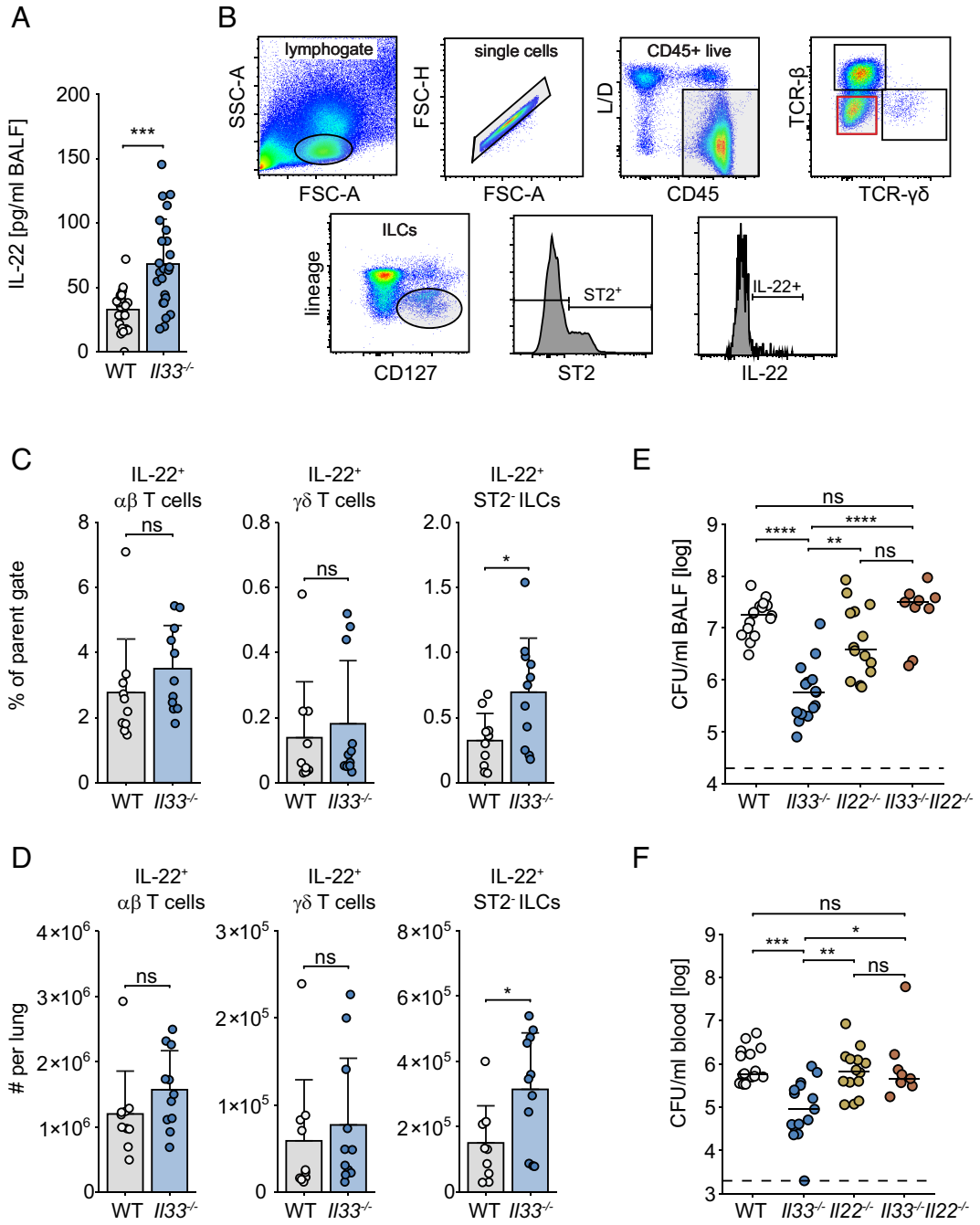

Fig. 3. The protective effect of IL-33 deficiency in pneumococcal infection is mediated by enhanced production of IL-22. (*A*) WT (n = 24) and *Il33*$^{-/-}$ (n = 24) mice were infected with *S. pneumoniae* and killed after 18 h, and levels of IL-22 in BALF were measured by the ELISA. (*B*) Representative gating strategy for analyzing IL-22^{+} lymphoid cells by FACS. (*C* and *D*) Frequency and absolute numbers of IL-22-producing lymphoid cells in the lungs of WT (n = 10) and *Il33*$^{-/-}$ mice (n = 11) 18 h after infection. (*E* and *F*) WT (n = 16), *Il33*$^{-/-}$ (n = 15), *Il22*$^{-/-}$ (n = 15), and *Il33*$^{-/-}$*Il22*$^{-/-}$ mice (n = 9) were infected for 48 h, and bacterial loads were determined in BALF (*E*) and blood (*F*). Data are shown as individual points. Bars represent mean + SD, lines represent the median, and the dashed line the lower detection limit. The Wilcoxon rank-sum test or Kruskal–Wallis test followed by Dunn's post hoc test was used if more than two groups were compared, ns = $P > 0.05$, *$P < 0.05$, **$P < 0.01$, ***$P < 0.001$, and ****$P < 0.0001$.

animals had to move several times from one vivarium to another within different institutional breeding facilities in Berlin. Unexpectedly, we observed that the phenotype of the *Il33*$^{-/-}$ mice in *S. pneumoniae* infection differed between the facilities: *Il33*$^{-/-}$ animals from several different vivaria with tendentially lower hygienic conditions (e.g., conventional caging instead of individually ventilated cages and/or free access for scientists instead of access only for the responsible animal caretakers) mostly retained their enhanced resistance to pneumococcal infection as compared to WT animals from the same vivaria. However, *Il33*$^{-/-}$ mice from other vivaria that tended to have a higher hygienic status were often less resistant to the infection and thus behaved similarly to WT animals (Fig. 4). These results led us to hypothesize that alterations in the gut microbiota, putatively dependent on interfacility environmental microbiome variabilities, influenced defense against *S. pneumoniae* infection in the lungs.

IL-33's Influence on Antibacterial Defense Depends on Its Modulatory Effect on the Microbiota. The microbiota has recently emerged as an important factor calibrating immune

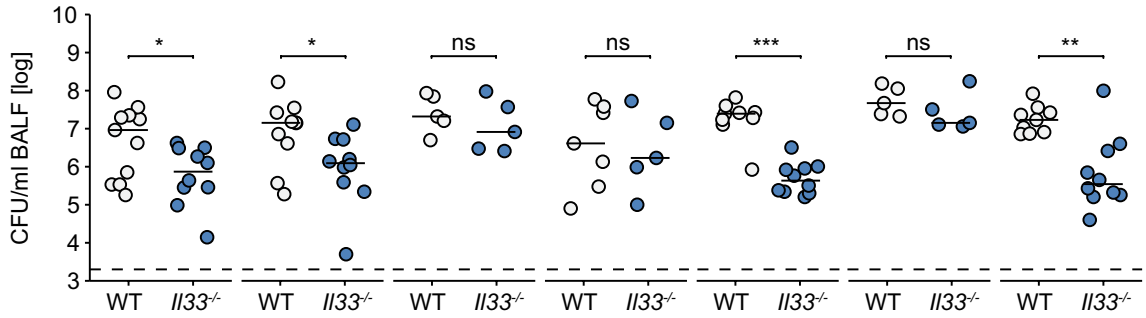

Fig. 4. *Il33*$^{-/-}$ mice from different vivaria vary in their susceptibility to *S. pneumoniae* infection. WT and *Il33*$^{-/-}$ mice from seven different animal vivaria were infected and killed after 48 h, and bacterial loads in BALF were assessed (n = 5 to 11 per group). Data are shown as individual points. Lines represent the median and the dashed line the lower detection limit. Wilcoxon rank-sum test, ns = $P > 0.05$, *$P < 0.05$, **$P < 0.01$, and ***$P < 0.001$.

responses and thereby influencing susceptibility to infection (4, 32–37). To investigate whether microbiota differences were indeed responsible for the variable resistance of *Il33*$^{-/-}$ animals to *S. pneumoniae* infection, we performed microbiota depletion, cohousing, and microbiota transfer experiments. When WT and *Il33*$^{-/-}$ mice from a vivarium normally breeding "resistant" *Il33*$^{-/-}$ animals were treated with antibiotics to deplete their microbiota, the difference in controlling *S. pneumoniae* infection and IL-22 production vanished (Fig. 5 *A* and *B*). Similarly, cohousing of WT and *Il33*$^{-/-}$ mice equalized their antibacterial defense (Fig. 5 *C* and *D*). Next, we assessed antibacterial defense in WT and IL-33-deficient animals transplanted with fecal material from WT and *Il33*$^{-/-}$ animals of two different vivaria. The results indicate that the resistance of IL-33-deficient mice to *S. pneumoniae* indeed depended on the gut microbiota (*SI Appendix*, Fig. S6). We then sequenced fecal samples of WT and *Il33*$^{-/-}$ mice from different vivaria as well as our cohoused animals to analyze their microbiota. Since, a reexamination of our data from the mice of the different vivaria provided evidence that only the *Il33*$^{-/-}$ but not the WT animals are influenced by the housing environment (*SI Appendix*, Fig. S7), we plotted the resistant *Il33*$^{-/-}$ mice against their corresponding WT controls as well as the "susceptible" *Il33*$^{-/-}$ and matching WT animals. While alpha diversities were comparable between samples of all WT and *Il33*$^{-/-}$ groups (Fig. 5*E*), taxonomic profiling revealed that the composition of samples from resistant *Il33*$^{-/-}$ animals was different compared to samples from susceptible *Il33*$^{-/-}$ mice and both WT controls. For example, the microbiota of resistant *Il33*$^{-/-}$ mice were characterized by higher relative abundance of various *Lactobacillus* spp. and lower abundance of *Saccharicrinis fermentans* and *Peptococcus niger* as compared to WT animals and to *Il33*$^{-/-}$ animals that did not show the resistant phenotype (Fig. 5*F*). As expected, cohousing of WT and *Il33*$^{-/-}$ animals normalized their intestinal microbial communities. Moreover, resistant *Il33*$^{-/-}$ mice also differed in terms of their gut virome as well as archean and eukaryotic communities from the other animal groups, and cohousing equalized these communities (*SI Appendix*, Fig. S8 *A*–*C*). Real-time PCR-based quantification of segmented filamentous bacteria (SFB), which are known to enhance IL-22 production (38, 39), did not reveal obvious differences between WT and *Il33*$^{-/-}$ animals, although the relative abundance of SFB in resistant *Il33*$^{-/-}$ mice was slightly higher compared to susceptible *Il33*$^{-/-}$ animals (*SI Appendix*, Fig. S8*D*). Finally, fecal material of mice from a unit with lower hygienic status rendered *Il33*$^{-/-}$ but not WT or *Il33*$^{-/-}$*Il22*$^{-/-}$ animals resistant to the infection (Fig. 5*G*), suggesting that a yet unidentified transferred microorganism was restricted in the gut of WT animals but blooms in *Il33*$^{-/-}$ animals to increase IL-22-dependent antibacterial defense in the lung. Together, our results demonstrate that IL-33 modifies the gut microbiota to influence IL-22-dependent resistance against *S. pneumoniae*.

Discussion

In our study, we describe a mechanism of bidirectional interaction between the immune system and the microbiota. The mechanism depends on both genetic and environmental factors and influences the efficacy of antibacterial immune defense and thus susceptibility to pneumonia. Specifically, we demonstrate that IL-33 regulates IL-22-dependent antibacterial defense in the lungs. This regulation of antibacterial defense is dependent on IL-33's modulatory influence on the microbiota and seems primarily apparent in mice that are kept in vivaria with tendentially lower hygienic conditions. Mice lacking ILC2s or IL-4Rα did not differ from their controls in response to *S. pneumoniae* infection, although all of them were housed in the same vivarium as the resistant *Il33*$^{-/-}$ animals. We speculate that one or several as yet unidentified microorganism(s), which we believe is/are primarily present in the low hygienic vivaria, is/are normally restricted in the gut by IL-33 but bloom(s) in *Il33*$^{-/-}$ animals to increase IL-22 production. SFB would have been a candidate for such a microorganism, as it is well known to enhance IL-22 production (38, 39). However, we did not detect increased abundance of SFB in our *Il33*$^{-/-}$ animals as compared to WT controls, thus making it unlikely that these bacteria are causally linked to the enhanced IL-22 production in our *Il33*$^{-/-}$ animals. To narrow down the identity of such a microbe, we compared the microbiota of resistant and susceptible IL-33-deficient mice and WT controls. Unfortunately, however, the number of taxa that differed in abundance was too large to test them individually in, for example, transplantation experiments to evaluate their ability to induce IL-22-dependent defense against *S. pneumoniae*.

The resistant phenotype of *Il33*$^{-/-}$ mice related to the altered microbiota was primarily observed when the animals were bred in vivaria that tended to have lower hygienic standards. Importantly, microbiota alterations in *Il33*$^{-/-}$ mice have also been described by others (40), suggesting that this is not a phenomenon observed specifically in our facilities. The previous study, however, found increased abundance of *Akkermansia muciniphila* in *Il33*$^{-/-}$ mice as compared to WT and *Il33*$^{+/-}$ littermates, whereas our *Il33*$^{-/-}$ mice differ in other taxa from their controls. Overall, we consider our results relevant since animals with lower hygienic status are likely to better reflect the physiological reality. This assumption is consistent with recent studies demonstrating that "wildlings", as mice

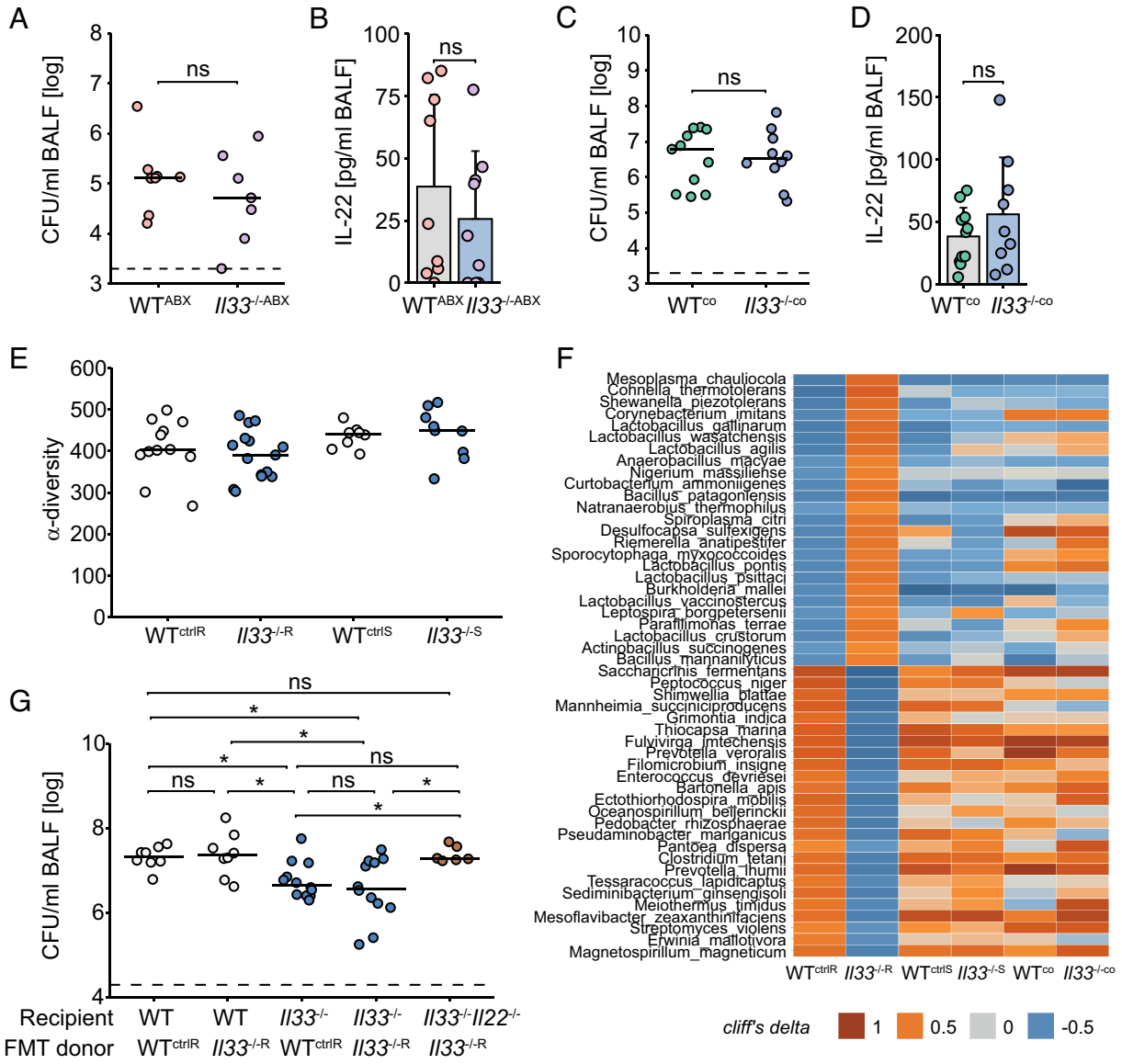

Fig. 5. IL-33's influence on antibacterial defense depends on its modulatory effect on the microbiota. (*A* and *B*) WT (n = 9) and *Il33*$^{-/-}$ mice (n = 9) were microbiota depleted by oral treatment with antibiotics, subsequently infected with 1 × 10^6 CFU/mouse, and killed after 48 h. Bacterial loads (*A*) and IL-22 levels (*B*) were assessed in BALF. (*C* and *D*) WT and *Il33*$^{-/-}$ mice were cohoused for 4 wk and infected for 48 h. Bacterial loads (*C*) and IL-22 levels (*D*) were assessed in BALF. (*A*–*D*) Data are shown as individual points, lines represent the median, the dashed line the lower detection limit, and bars represent mean + SD. Wilcoxon rank-sum test, ns = $P > 0.05$. (*E*) Alpha diversity of microbiota samples from *Il33*$^{-/-}$ animals with resistant (*Il33*$^{-/-R}$) and susceptible phenotype (*Il33*$^{-/-S}$) and corresponding controls (WT^{ctrlR} and WT^{ctrlS}) is shown. (*F*) Heatmap of shotgun-sequenced bacterial microbiota derived from resistant (n = 15) and susceptible *Il33*$^{-/-}$ (n = 13), their respective controls (for WT^{ctrlR} n = 15 and WT^{ctrlS} n = 12), and cohoused WT (n = 11) and *Il33*$^{-/-}$ mice (n = 10). Cliff's delta was applied to visualize most differential effect sizes between *Il33*$^{-/-R}$ and WT^{ctrlR}. (*G*) WT, *Il33*$^{-/-}$, and *Il33*$^{-/-}$*Il22*$^{-/-}$ mice were treated orally with an antibiotic cocktail to deplete their own microbiota. Afterward, mice were transplanted with fecal samples derived from WT^{ctrlR} or *Il33*$^{-/-R}$ animals. After a reconstitution time of 18 d, mice were intranasally infected with *S. pneumoniae*. Data are shown as individual points (n = 8 for WT^{ctrlR} > WT, n = 8 for *Il33*$^{-/-R}$ > WT, n = 12 for WT^{ctrlR} > *Il33*$^{-/-}$, n = 12 for *Il33*$^{-/-R}$ > *Il33*$^{-/-}$ and n = 6 for *Il33*$^{-/-R}$ > *Il33*$^{-/-}$*Il22*$^{-/-}$). Kruskal–Wallis test followed by Dunn's post hoc test; ns = $P > 0.05$ and *$P < 0.05$.

whose hygiene status could be considered particularly low, mimic human immune responses better than SPF animals kept under high hygienic conditions (41, 42). Moreover, our analyses of a large cohort of patients with community-acquired pneumococcal pneumonia and age- and sex-matched controls revealed an association between pneumococcal pneumonia and carriage of SNP alleles previously linked to altered IL-33 signaling (22–24). These results provide preliminary evidence that IL-33 signaling may also influence susceptibility to bacterial lung infections in humans.

Two elegant studies have recently demonstrated that lung epithelial IL-33 imprints an anti-inflammatory "M2-like" phenotype in AMs by acting through ILC2s, basophils, and IL-13 (43, 44). In addition, IL-13-deficient mice were shown to exhibit enhanced resistance to bacterial infection (43). In contrast to these studies, we did not observe decreased susceptibility of mice lacking the alpha chain of the IL-4 receptor, which is required for IL-4 and IL-13 signaling. We speculate that differences in the infection models and/or the microbiome of the animals used could explain this discrepancy.

Overall, our study provides insights into how environmental and genetic factors influence the microbiota, and how this affects antimicrobial immune defense and susceptibility to infection. Future work is needed to identify the specific microbes that we believe are normally controlled by IL-33 in the gut and regulate the production of IL-22 in the lung. Moreover, the mechanism of how IL-33 influences the intestinal microbiota is still unknown and warrants further investigations.

Materials and Methods

Study Approval. All animal experiments were carried out in adherence to the German Animal Welfare Act (Tierschutzgesetz, TierSchG) and to the Federation of European Laboratory Animal Science Association guidelines, following approval by the responsible institutional (Charité–Universitätsmedizin Berlin) and governmental animal welfare authorities (LAGeSo Berlin, approval IDs G0266/11, G0365/12, G0227/16, G0080/18, G0010/22, and T0014/12). Samples from the pneumococcal pneumonia patients were provided by the CAPNETZ foundation (45). This prospective multicenter study (German Clinical Trials Register: DRKS00005274) was approved by the ethical review board of each participating clinical center (Reference number of leading Ethics Committee "Medical Faculty of Otto-von-Guericke-University in Magdeburg": 104/01 and "Medical School Hannover": 301/2008) and was performed in accordance with the Declaration of Helsinki. All patients provided written informed consent prior to enrollment in the study.

Mice. *Il33*$^{-/-}$ mice (46), kindly provided by Hirohisa Saito (National Research Institute for Child Health and Development, Tokyo, Japan), were crossed with *Il22*$^{-/-}$ (47) mice to generate a double knockout line *Il33*$^{-/-}$*Il22*$^{-/-}$. *Nmur1*$^{iCre\text{-}eGFP}$ *Id2* $^{fl/fl}$ mice and *Id2* $^{fl/fl}$ littermate controls were recently described (28, 48). *Il4ra*$^{-/-}$ mice were described in ref. 49. *Il1rl1*$^{-/-}$ mice (50) were kindly provided by Andrew McKenzie (MRC Laboratory of Molecular Biology, Cambridge, UK). *P2rx7*$^{-/-}$ (51) and *P2ry6*$^{-/-}$ (52) mice were described before and were kindly provided by Marco Idzko (University Hospital Vienna AKH, Medical University of Vienna, Vienna, Austria). All mice were on a C57BL/6 background and bred in the animal facility of the Forschungseinrichtungen für experimentelle Medizin (FEM), Charité–Universitätsmedizin Berlin. *Il22*$^{-/-}$, *Il33*$^{-/-}$*Il22*$^{-/-}$, *Nmur1*$^{iCre\text{-}eGFP}$*Id2*$^{fl/fl}$, *Id2*$^{fl/fl}$, *Il1rl1*$^{-/-}$, and *Il4ra*$^{-/-}$ mice were bred in the same vivaria that generated resistant *Il33*$^{-/-}$ animals. For all experiments, age-matched mice, usually aged 8 to 12 wk, were used.

***S. pneumoniae* Infection.** The murine in vivo model of pneumococcal pneumonia has previously been described (53, 54). Briefly, we used the serotype 3 strain of *S. pneumoniae* PN36 (NCTC7978), kindly provided by Sven Hammerschmidt (Ernst-Moritz-Arndt-Universität Greifswald, Germany). Bacteria were plated on Columbia agar plates (5% sheep blood) and harvested after 9 h of incubation at 37 °C + 5% CO_2, single colonies were picked, and optical density was measured at OD_{600nm} and adjusted for the infection dose. Mice were anesthetized with an intraperitoneal (i.p.) injection of 80 mg/kg ketamine and 25 mg/kg xylazine and transnasally inoculated with 5×10^6 colony-forming units (CFU) *S. pneumoniae* in 20 μL PBS per mouse. Sham-infected mice received 20 μL phosphate buffered saline (PBS). Following infection, temperature and weight were measured every 12 h to monitor the clinical course of disease. At the indicated time points, mice received an i.p. injection of 160 mg/kg ketamine and 75 mg/kg xylazine and were killed 12, 18, 36, or 48 h postinfection by final blood withdrawal. Blood was centrifuged, serum was collected, and the lungs were perfused with 5 mL of PBS. All organs of interest were either snap-frozen in liquid nitrogen or processed immediately. Bronchoalveolar lavage was performed by lavaging the lungs twice with 800 μL PBS containing protease inhibitors. Both fractions were centrifuged, and BALF was collected. The pelleted cells were combined and used for subsequent flow cytometry analyses. The bacterial loads were determined in BALF before centrifugation of blood and spleen by plating them on blood agar plates and overnight incubation.

Generation of Chimera Mice. Mice (10 to 12 wk old) were radiated with a dose of 10 Gy and 24 h later transplanted with 5×10^6 freshly isolated bone marrow cells of either WT or *Il33*$^{-/-}$ congenic (CD45.1$^+$) mice. Donor cells were first reconstituted in 200 μL PBS and then intravenously injected into recipient mice. To prevent infections, recipient mice received 0.01% enrofloxacin ad libitum for 4 wk starting 1 d before radiation. After 10 wk of reconstitution, mice were infected with *S. pneumoniae,* and bacterial defense was investigated.

In Vitro Infection. Bone marrow–derived macrophages (BMM), AEC, or whole lung suspensions were isolated from WT mice and infected in vitro with 1×10^6 CFU *S. pneumoniae* (D39), and the supernatant was harvested 16 h (BMM and AEC) and 24 h (murine lung homogenate) postinfection. Protein levels of uric acid, ATP, and IL-33 were measured via the ELISA (eBioscience, R&D Systems) according to the manufacturer's instructions.

Intratracheal Treatment of Mice. WT mice were intratracheally treated with PBS (control), uricase (0.073 U/per mouse), apyrase (0.32 U/per mouse), suramin (32 μM/per mouse), or pyridoxal-phosphate-6-azophenyl-2′,4′-disulfonic acid (32 μM/per mouse) dissolved in 25 μL PBS immediately before *S. pneumoniae* infection and 24 h after. For the treatment 24 h postinfection, mice were orotracheally intubated with a laryngoscope, and the solution was then applied into the lungs with a microsprayer. Mice were killed after 48 h, and bacterial burden was quantified.

Intranasal and i.p. Treatment of Mice. Animals were intranasally treated with 1 μg rIL-22 (R&D Systems) at the time of infection and additionally intraperitoneally with 1 μg rIL-22 at 24 h postinfection. The control animals received PBS.

Real-Time qPCR. DNA extraction was carried out utilizing the ZymoBIOMICS DNA extraction kit (Zymo), following the instructions provided by the manufacturer. Gene expression analysis was conducted using 1× SYBR Green Master Mix, following the manufacturer's guidelines from Applied Biosystems. The primer sequences for qRT-PCR were the following: SFB_forward: 5′-GACGCTGAGGCATGAGAGCAT-3′, SFB_reverse: 5′-GACGGCACGGATTGTTATTCA-3′.

Flow Cytometry. The cell pellets obtained from both lavages were pooled in 1 mL PBS and analyzed by flow cytometry. The relative and absolute number of AMs ($CD45^+$ $CD11b^-$ Siglec-F^+), recruited PMNs ($CD45^+$ $CD11b^+$ $Ly6G^+$), and inflammatory monocytes ($CD45^+$ $Ly6G^-$ $CD11b^+$ $Ly6C^{++}$) were determined. Moreover, the lungs were perfused, isolated, cut into pieces, and incubated in 5 mL RPMI 1640 (+5% FCS) containing collagenase (150 U/mL) and DNase (1,500 U/mL) for 40 min at 37 °C while shaking. Digested lung cells were passed through a 70 μm cell strainer, and red blood cells were lysed. Cells were solved in FACS buffer (PBS + 2% FCS) and subsequently stained for flow cytometry. Following populations were measured in the lungs: ILC ($CD45^+$ $CD127^+$ $CD90^+$ $TCR\beta^-$ $TCR\gamma\delta^-$ $CD3^-$ $CD19^-$ $Fc\varepsilon RI\alpha^-$ $Ly6G^-$ $CD5^-$ $NK1.1^-$ Siglec-F^-), ILC2 ($CD45^+$ $CD127^+$ $CD90^+$ $CD3^-$ $CD19^-$ $Fc\varepsilon RI\alpha^-$ $Ly6G^-$ $CD5^-$ $NK1.1^-$ $GATA3^+$), αβ T cells ($CD45^+$ $CD3^+$ $TCR\beta^+$ $TCR\gamma\delta^-$), and γδ T cells ($CD45^+$ $CD3^+$ $TCR\beta^-$ $TCR\gamma\delta^+$). For intracellular staining, the lungs were prepared as described, left unstimulated, or stimulated with 50 ng/mL phorbol-12-myristate-13-acetate, 1 μg/mL ionomycin, and 1 μg/mL brefeldin A (all Sigma-Aldrich) for 5 h at 37 °C + 5% CO_2. For the process of permeabilization, either FoxP3 Fix/Perm kit (BioLegend) or 2% paraformaldehyde (PFA) was used. ILC2 were sorted for $CD45^+$ $CD3^-$ $CD19^-$ $Ly6G^-$ $FceRIa^-$ $CD5^-$ $NK1.1^-$ $CD127^+$ $CD90^+$ $ST2^+$ and further processed for bulk RNA sequencing.

ELISA. Quantification of cytokine and chemokine levels in BALF was conducted by using a commercial multiplex assay (ProcartaPlex, Thermo Fisher) and commercially available single-cytokine ELISA kits (eBioscience, R&D Systems).

ScRNAseq. After infection and preparation, the lungs were perfused with 5 mL PBS followed by 2 mL dispase (5,000 U/mL, Corning). Then, 700 μL dispase was applied intratracheally, followed by 500 μL lukewarm 1% low melt agarose. The lungs were then removed and transferred into digestion medium (PBS + 5% FCS + 2 μg/mL Actinomycin D + 2 mg/mL collagenase + 0.5 mg/mL DNase), cut into pieces, and incubated for 30 min at 37 °C at 125 rpm in a shaker. Lung homogenates of each group were combined and filtered through a 70 μm cell strainer, red blood cells were lysed, and cells were counted using a hemocytometer and dead cells were removed with a magnetic bead–based dead cell removal kit according to the manufacturer's instructions (EasySep STEMCELL Technologies). Following lung digestion, 1/4 of the cell suspension was sorted for $CD45^+$ $CD3^-$ $CD19^-$ $Ly6G^-$ $FceRIa^-$ $CD5^-$ $NK1.1^-$ $CD127^+$ $CD90^+$ ILCs and spiked back into the whole lung single-cell solution. Then, cells were loaded into the Chromium Controller (10×). Single Cell 5′ reagent kit v2 was used for reverse transcription, cDNA amplification, and library construction, followed by the detailed protocol provided by 10× Genomics. The generated libraries were sequenced on a NovaSeq 6000 S4 flowcell type with 200 cycles with 30,000 cells per lane and 4 lanes in total, targeting 2,500 million reads/lane. The reads were aligned to the reference genome provided by 10× Genomics (Mouse reference mm10), and a digital gene expression matrix was generated to record the number of unique molecular identifiers for each gene in every cell. Quality metrics were applied to the count matrices, and thresholds were set for the

number of genes (>150 and <4,000) and the percentage of mitochondrial reads (less than 10%). For data integration, variable feature finding, data scaling, and principal component analysis (PCA) calculation based on highly variable genes, the standard pipeline of the Seurat package (version 4.2.0) was used (55). In case of batch effects, the Harmony (56) or SoupX (57) package was utilized for correction. The functions RunUMAP(), FindNeighbours(), and FindClusters() were employed to reduce dimensions and find Shared Nearest Neighbours in the dataset. To calculate differential gene expression, the Seurat function FindMarkers() was used.

Fecal DNA Extraction and Shotgun Sequencing. Mouse fecal samples derived from seven vivaria were collected before infection and stored at −80 °C until further use. For the DNA extraction, a DNA Miniprep Kit from Zymo Research (#D4300) was used, and the purity and concentration of the DNA were measured using a NanoDrop™ 2000 (Thermo Fisher). Library prep and sequencing of the bacterial DNA were performed by Eurofins Genomics (Ebersberg, Germany) using an Illumina NovaSeq 6000, with 10 million reads and paired-end sequencing (2 × 150 bp). After sequencing, preprocessing was conducted by Eurofins genomics. Poor-quality bases, adapters, and primers were removed before proceeding to the removal of host sequences. Taxonomic profiling was conducted by using the NCBI database of bacterial, archaeal, fungal, protozoan, and viral genomes. FASTQ files were generated, and a table containing normalized reads for each domain, phylum, class, order, family, genus, and species was provided. This table was then loaded into R and used for subsequent analyses.

Bulk RNA Sequencing. To prepare mouse lungs for RNA bulk sequencing, the infected lungs were digested and FACS-sorted for ILC2 as described. RNA was isolated using the Direct-Zol Microprep Kit (Zymo Research, Cat#R2061). Library preparation was done with Takara SMARTer stranded Total RNA-Seq Kit v3–Pico Input, and library was sequenced on a NovaSeq 6000 SP targeting 400 million reads. Adapter sequences were removed from sequencing reads with Cutadapt (v3.7), and their quality was assessed with FASTQC (v0.11.9). Subsequently, reads were input into SeA-SnaP: (Se)q (A)nalysis (Sna)kemake (P)ipeline (https://github.com/bihealth/seasnap-pipeline). Briefly, reads were mapped with STAR aligner (v2.7.3a) to the mm10/GRCm38 mouse genome using GENCODE annotation version M12. Next, featureCounts (v2.0.0) was used to count reads in exons and generate a read count table. Differential expression analysis was carried out with DeSeq2 (v1.34.0) (56) Differentially expressed genes (adjusted P value < 0.1) were subjected to gene set enrichment analysis using the fgsea package (version 1.16.0).

Microbiota Depletion. To study the effects of antibiotic treatment on the gut microbiota of mice, 8- to 9-wk-old mice were housed in sterile cages and treated orally with a combination of imipenem (250 mg/L; Fresenius Kabi), metronidazole (1 g/L; Braun), vancomycin (500 mg/L; HIKMA Pharma), ciprofloxacin (200 mg/L; Fresenius Kabi), and ampicillin (1 g/L; Ratiopharm) in the drinking water ad libitum for a period of 6 wk (ABX mice) as described earlier (58). Fecal samples were collected weekly for analysis of fungal outgrowth and depletion of the gut microbiota, using bacterial and fungal cultivation on agar plates. Any mice that showed fungal outgrowth were excluded from the study.

Murine Fecal Microbiota Transplantation. Microbiota-depleted mice were handled under strict aseptic conditions to avoid any contaminations and assure successful microbiota depletion. Four days before the fecal microbiota transplantation, the antibiotic treatment was withdrawn and replaced by autoclaved water (ad libitum). Mice were transplanted with fecal samples derived from WT or *Il33*$^{-/-}$ mice. Samples were collected, pooled by genotype and vivarium, resuspended in sterile PBS, and filtered using a 70 μM cell strainer. Then, 300 μL of the fecal transplant sample was administered to WT, *Il33*$^{-/-}$, or *Il33*$^{-/-}$*Il22*$^{-/-}$ mice three times on three consecutive days by oral gavage. Mice were infected with *S. pneumoniae* 8 to 19 d after transplantation.

SNP Analysis. Samples were provided by the CAPNETZ competence network, a German multicenter prospective cohort study for CAP (45). The control groups consisted of a subgroup of healthy adults of similar age and sex distribution from the PolSenior program, an interdisciplinary project, designed to evaluate the health and socioeconomic status of the Polish Caucasians aged ≥65 y (59). DNA Genotyping of rs1420101, rs7044343, rs9500880, and rs1921622 was conducted by PCR utilizing fluorescent-labeled hybridization FRET probes followed by melting curve analysis in a LightCycler 480 (Roche Diagnostics). The following probes and primers were used: rs1420101: f-primer: TAgTTggTgTCAgAgTTTCTgCAA, r-primer: TgAAgTgACTTACTCAAggCCA, anchor probe: LC640 CCAATgAgTATTACTAAAgATTAAgCTCTT-PH, sensor probe: AAAgCCTCTCATTAAACTTTgAA-FL; rs7044343: f-primer: AggAATgAATATTgggTgACACTATg, r-primer: TACCCAAgTTCAAgAggCACTg, anchor probe: LC640 TCCTgTCTgCATgTAAAgCCACTC-PH, sensor probe: ggTTACTTCTCAgggCATCA-FL; rs9500880: f-primer: TTCAggAAATTAgAggTCTAATgTAA, r-primer: CTgCAgAgACATgCCAAAgACA, anchor probe: LC640 gACgAAAgCATTCTTAAATCTgATATTC-PH, sensor probe: TgATTTCTAgTTCCACACTTATgA-FL; rs1921622: f-primer: CACCAggATAACTCTgCCAC, r-primer: TAAATTTgCAAATgTTTCACCAAC, anchor probe: LC640 gCCATAggCACTAgCTgAAATAC-PH, sensor probe: TAAAAATTgATgAATTTTgTTCTgg-FL.

Data Analysis and Statistics. Data analysis was performed using R, version 4.2.1. The Wilcoxon rank-sum test was used for the comparison of two groups. If more than two groups were compared, the Kruskal–Wallis test, followed by Dunn's post hoc test, was utilized. SNP allele frequencies were analyzed using Fisher's exact test.

Data, Materials, and Software Availability. RNAseq and microbiota shotgun sequencing data have been deposited in GEO Repository GSE236344 (60).

ACKNOWLEDGMENTS. We are grateful to all patients for consenting to biosampling and data collection. We would like to thank Ulrike Fiebiger, Alexandra Bittroff-Leben, Katrin Heiden, and the staff of the animal facility of the FEM of the Charité–Universitätsmedizin Berlin for excellent technical assistance, animal breeding, and generation of secondary abiotic mice. We also would like to thank Dr. Birgitt Gutbier and Dr. Katrin Reppe for her help with our animal experiments. We are grateful to the Benjamin Franklin Flow Cytometry Facility for support in cell sorting. BFFC is supported by DFG Instrument Grants INST 335/597-1 FUGG und INST 335/777-1 FUGG. This work was supported in parts by the German Research Foundation (SFB-TR84 A1 to A.D. and B.O., SFB1444 TP11 to A.D., OP86/13-1 to B.O., and TRR 167–259373024, FOR2599–322359157, TRR 241–375876048, SPP1937–KL 2963/2-1 and KL 2963/3-1 to C.S.N.K.), the German Federal Ministry of Education and Research (MAPVAP FKZ 01KI2124 to M.W. and B.O.), and the European Research Council (Starting Grant, ERCEA; 803087 to C.S.N.K. and Advanced Grant, 101055309 - ILCADAPT to A.D.). A.D. is the Einstein Professor of Microbiology (Einstein Foundation Berlin).

Author affiliations: [a]Department of Infectious Diseases, Respiratory Medicine and Critical Care, Charité–Universitätsmedizin Berlin, Corporate Member of Freie Universität Berlin and Humboldt-Universität zu Berlin, Berlin 13353, Germany; [b]Institute of Microbiology, Infectious Diseases and Immunology, Charité–Universitätsmedizin Berlin, Corporate Member of Freie Universität Berlin and Humboldt-Universität zu Berlin, Berlin 12203, Germany; [c]German Rheumatism Research Center, a Leibniz Institute, Berlin 10117, Germany; [d]Core Unit Bioinformatics, Berlin Institute of Health at Charité, Berlin 10117, Germany; [e]Research Group Infection Immunology, Institute of Medical Microbiology and Hospital Hygiene, Health Campus Immunology, Infectiology and Inflammation, Otto-von-Guericke-University, Magdeburg 39120, Germany; [f]Research Group Immune Regulation, Helmholtz Centre for Infection Research, Braunschweig 38124, Germany; [g]Department of Human Epigenetics, Mossakowski Medical Research Institute, Polish Academy of Sciences, Warsaw 02-106, Poland; [h]Department of Geriatrics and Gerontology, Medical Centre of Postgraduate Education, Warsaw 01-813, Poland; [i]German center for lung research (DZL), Berlin 13353, Germany; [j]Experimental Immunology and Osteoarthritis Research, Department of Rheumatology and Clinical Immunology, Charité–Universitätsmedizin Berlin, Corporate member of Freie Universität Berlin and Humboldt-Universität zu Berlin, Berlin 10117, Germany; and [k]Pitzer Laboratory of Osteoarthritis Research, German Rheumatism Research Center, a Leibniz Institute, Berlin 10117, Germany

1. G. L. Collaborators, Estimates of the global, regional, and national morbidity, mortality, and aetiologies of lower respiratory tract infections in 195 countries: A systematic analysis for the Global Burden of Disease Study 2015. *Lancet Infect. Dis.* **17**, 1133–1161 (2017).
2. N. Johansson, M. Kalin, A. Tiveljung-Lindell, C. G. Giske, J. Hedlund, Etiology of community-acquired pneumonia: Increased microbiological yield with new diagnostic methods. *Clin. Infect. Dis.* **50**, 202–209 (2010).
3. S. M. Huijts *et al.*, Diagnostic accuracy of a serotype-specific antigen test in community-acquired pneumonia. *Eur. Respir. J.* **42**, 1283–1290 (2013).
4. C. Thibeault, N. Suttorp, B. Opitz, The microbiota in pneumonia: From protection to predisposition. *Sci. Transl. Med.* **13**, eaba0501 (2021).
5. J. N. Weiser, D. M. Ferreira, J. C. Paton, Streptococcus pneumoniae: Transmission, colonization and invasion. *Nat. Rev. Microbiol.* **16**, 355–367 (2018).

6. B. Opitz, V. van Laak, J. Eitel, N. Suttorp, Innate immune recognition in infectious and noninfectious diseases of the lung. *Am. J. Respir. Crit. Care Med.* **181**, 1294–1309 (2010).
7. S. Akira, S. Uematsu, O. Takeuchi, Pathogen recognition and innate immunity. *Cell* **124**, 783–801 (2006).
8. A. Iwasaki, E. F. Foxman, R. D. Molony, Early local immune defences in the respiratory tract. *Nat. Rev. Immunol.* **17**, 7–20 (2017).
9. S. J. Aujla *et al.*, IL-22 mediates mucosal host defense against Gram-negative bacterial pneumonia. *Nat. Med.* **14**, 275–281 (2008).
10. S. L. Sanos *et al.*, RORgammat and commensal microflora are required for the differentiation of mucosal interleukin 22-producing NKp46+ cells. *Nat. Immunol.* **10**, 83–91 (2009).
11. Y. Zheng *et al.*, Interleukin-22 mediates early host defense against attaching and effacing bacterial pathogens. *Nat. Med.* **14**, 282–289 (2008).
12. L. A. Zenewicz *et al.*, Interleukin-22 but not interleukin-17 provides protection to hepatocytes during acute liver inflammation. *Immunity* **27**, 647–659 (2007).
13. M. O. Jakob *et al.*, ILC3s restrict the dissemination of intestinal bacteria to safeguard liver regeneration after surgery. *Cell Rep.* **42**, 112269 (2023).
14. G. Trevejo-Nunez, W. Elsegeiny, P. Conboy, K. Chen, J. K. Kolls, Critical role of IL-22/IL22-RA1 signaling in pneumococcal pneumonia. *J. Immunol.* **197**, 1877–1883 (2016).
15. L. Van Maele *et al.*, Activation of Type 3 innate lymphoid cells and interleukin 22 secretion in the lungs during Streptococcus pneumoniae infection. *J. Infect. Dis.* **210**, 493–503 (2014).
16. K. D. Hebert *et al.*, Targeting the IL-22/IL-22BP axis enhances tight junctions and reduces inflammation during influenza infection. *Mucosal Immunol.* **13**, 64–74 (2020).
17. T. Ito *et al.*, IL-22 induces Reg3gamma and inhibits allergic inflammation in house dust mite-induced asthma models. *J. Exp. Med.* **214**, 3037–3050 (2017).
18. G. Y. Chen, G. Nunez, Sterile inflammation: Sensing and reacting to damage. *Nat. Rev. Immunol.* **10**, 826–837 (2010).
19. F. Y. Liew, J. P. Girard, H. R. Turnquist, Interleukin-33 in health and disease. *Nat. Rev. Immunol.* **16**, 676–689 (2016).
20. M. Peine, R. M. Marek, M. Lohning, IL-33 in T cell differentiation, function, and immune homeostasis. *Trends Immunol.* **37**, 321–333 (2016).
21. G. K. Dwyer, L. M. D'Cruz, H. R. Turnquist, Emerging functions of IL-33 in homeostasis and immunity. *Annu. Rev. Immunol.* **40**, 15–43 (2022).
22. E. D. Gordon *et al.*, IL1RL1 asthma risk variants regulate airway type 2 inflammation. *JCI Insight* **1**, e87871 (2016).
23. J. E. Ho *et al.*, Common genetic variation at the IL1RL1 locus regulates IL-33/ST2 signaling. *J. Clin. Invest.* **123**, 4208–4218 (2013).
24. J. Angeles-Martinez *et al.*, The rs7044343 polymorphism of the interleukin 33 gene is associated with decreased risk of developing premature coronary artery disease and central obesity, and could be involved in regulating the production of IL-33. *PLoS One* **12**, e0168828 (2017).
25. D. F. Gudbjartsson *et al.*, Sequence variants affecting eosinophil numbers associate with asthma and myocardial infarction. *Nat. Genet.* **41**, 342–347 (2009).
26. N. E. Reijmerink *et al.*, Association of IL1RL1, IL18R1, and IL18RAP gene cluster polymorphisms with asthma and atopy. *J. Allergy Clin. Immunol.* **122**, 651–654.e8 (2008).
27. S. Falahi *et al.*, Association between IL-33 gene polymorphism (Rs7044343) and risk of allergic rhinitis. *Immunol. Invest.* **51**, 29–39 (2022).
28. K. J. Jarick *et al.*, Non-redundant functions of group 2 innate lymphoid cells. *Nature* **611**, 794–800 (2022).
29. A. M. Tsou *et al.*, Neuropeptide regulation of non-redundant ILC2 responses at barrier surfaces. *Nature* **611**, 787–793 (2022).
30. W. Ouyang, A. O'Garra, IL-10 family cytokines IL-10 and IL-22: From basic science to clinical translation. *Immunity* **50**, 871–891 (2019).
31. G. F. Sonnenberg, L. A. Fouser, D. Artis, Border patrol: Regulation of immunity, inflammation and tissue homeostasis at barrier surfaces by IL-22. *Nat. Immunol.* **12**, 383–390 (2011).
32. E. Ansaldo, T. K. Farley, Y. Belkaid, Control of immunity by the microbiota. *Annu. Rev. Immunol.* **39**, 449–479 (2021).
33. T. P. Wypych, L. C. Wickramasinghe, B. J. Marsland, The influence of the microbiome on respiratory health. *Nat. Immunol.* **20**, 1279–1290 (2019).
34. T. B. Clarke *et al.*, Recognition of peptidoglycan from the microbiota by Nod1 enhances systemic innate immunity. *Nat. Med.* **16**, 228–231 (2010).
35. O. H. Robak *et al.*, Antibiotic treatment-induced secondary IgA deficiency enhances susceptibility to Pseudomonas aeruginosa pneumonia. *J. Clin. Invest.* **128**, 3535–3545 (2018).
36. T. J. Schuijt *et al.*, The gut microbiota plays a protective role in the host defence against pneumococcal pneumonia. *Gut* **65**, 575–583 (2016).
37. S. C. Ganal *et al.*, Priming of natural killer cells by nonmucosal mononuclear phagocytes requires instructive signals from commensal microbiota. *Immunity* **37**, 171–186 (2012).
38. I. I. Ivanov *et al.*, Induction of intestinal Th17 cells by segmented filamentous bacteria. *Cell* **139**, 485–498 (2009).
39. H. L. Klaasen *et al.*, Apathogenic, intestinal, segmented, filamentous bacteria stimulate the mucosal immune system of mice. *Infect. Immun.* **61**, 303–306 (1993).
40. A. Malik *et al.*, IL-33 regulates the IgA-microbiota axis to restrain IL-1alpha-dependent colitis and tumorigenesis. *J. Clin. Invest.* **126**, 4469–4481 (2016).
41. S. P. Rosshart *et al.*, Laboratory mice born to wild mice have natural microbiota and model human immune responses. *Science* **365**, eaaw4361 (2019).
42. S. P. Rosshart *et al.*, Wild mouse gut microbiota promotes host fitness and improves disease resistance. *Cell* **171**, 1015–1028.e13 (2017).
43. S. Saluzzo *et al.*, First-breath-induced type 2 pathways shape the lung immune environment. *Cell Rep.* **18**, 1893–1905 (2017).
44. M. Cohen *et al.*, Lung single-cell signaling interaction map reveals basophil role in macrophage imprinting. *Cell* **175**, 1031–1044.e18 (2018).
45. T. Welte, N. Suttorp, R. Marre, CAPNETZ-community-acquired pneumonia competence network. *Infection* **32**, 234–238 (2004).
46. K. Oboki *et al.*, IL-33 is a crucial amplifier of innate rather than acquired immunity. *Proc. Natl. Acad. Sci. U.S.A.* **107**, 18581–18586 (2010).
47. K. Kreymborg *et al.*, IL-22 is expressed by Th17 cells in an IL-23-dependent fashion, but not required for the development of autoimmune encephalomyelitis. *J. Immunol.* **179**, 8098–8104 (2007).
48. F. Niola *et al.*, Id proteins synchronize stemness and anchorage to the niche of neural stem cells. *Nat. Cell Biol.* **14**, 477–487 (2012).
49. M. Barner, M. Mohrs, F. Brombacher, M. Kopf, Differences between IL-4R alpha-deficient and IL-4-deficient mice reveal a role for IL-13 in the regulation of Th2 responses. *Curr. Biol.* **8**, 669–672 (1998).
50. M. J. Townsend, P. G. Fallon, D. J. Matthews, H. E. Jolin, A. N. McKenzie, T1/ST2-deficient mice demonstrate the importance of T1/ST2 in developing primary T helper cell type 2 responses. *J. Exp. Med.* **191**, 1069–1076 (2000).
51. I. P. Chessell *et al.*, Disruption of the P2X7 purinoceptor gene abolishes chronic inflammatory and neuropathic pain. *Pain* **114**, 386–396 (2005).
52. I. Bar *et al.*, Knockout mice reveal a role for P2Y6 receptor in macrophages, endothelial cells, and vascular smooth muscle cells. *Mol. Pharmacol.* **74**, 777–784 (2008).
53. J. S. Ruiz-Moreno *et al.*, The cGAS/STING pathway detects streptococcus pneumoniae but appears dispensable for antipneumococcal defense in mice and humans. *Infect. Immun.* **86** (2018).
54. A. Rabes *et al.*, The C-type lectin receptor Mincle binds to Streptococcus pneumoniae but plays a limited role in the anti-pneumococcal innate immune response. *PLoS One* **10**, e0117022 (2015).
55. Y. Hao *et al.*, Integrated analysis of multimodal single-cell data. *Cell* **184**, 3573–3587.e29 (2021).
56. I. Korsunsky *et al.*, Fast, sensitive and accurate integration of single-cell data with Harmony. *Nat. Methods* **16**, 1289–1296 (2019).
57. M. D. Young, S. Behjati, SoupX removes ambient RNA contamination from droplet-based single-cell RNA sequencing data. *Gigascience* **9**, giaa151 (2020).
58. M. M. Heimesaat *et al.*, Gram-negative bacteria aggravate murine small intestinal Th1-type immunopathology following oral infection with Toxoplasma gondii. *J. Immunol.* **177**, 8785–8795 (2006).
59. P. Bledowski *et al.*, Medical, psychological and socioeconomic aspects of aging in Poland: Assumptions and objectives of the PolSenior project. *Exp. Gerontol.* **46**, 1003–1009 (2011).
60. I. Röwekamp *et al.*, Raw data for IL-33 controls IL-22-dependent antibacterial defense by modulating the microbiota. NCBI GEO. https://www.ncbi.nlm.nih.gov/geo/query/acc.cgi?acc=GSE236344. Deposited 3 July 2023.